ELSEVIER

Spectrochimica Acta Part A 54 (1998) 1811–1818

SPECTROCHIMICA ACTA PART A

Vibrational spectra and structures of zinc carboxylates II. Anhydrous zinc acetate and zinc stearate

Tsutomu Ishioka *, Youko Shibata, Mizuki Takahashi, Isao Kanesaka

Department of Chemistry, Faculty of Science, Toyama University, Gofuku, Toyama 930-8555, Japan

Received 16 October 1997; received in revised form 8 March 1998; accepted 8 March 1998

Abstract

A normal mode analysis was carried out for a monoclinic anhydrous zinc acetate crystal in which the acetate groups had bridging bidentate coordination forms, and spectral assignments were made. Based on the assignments, a relation between the coordination structure of the carboxylate groups around the zinc atom and the vibrational frequencies of the carboxylate rocking mode was found. This relation was applied to zinc stearate to determine its coordination form, and we found that zinc stearate had a bridging bidentate form.

Keywords: Anhydrous zinc acetate; Zinc stearate; Vibrational spectra

1. Introduction

Monoclinic anhydrous zinc acetate has a crystal structure in which a zinc atom is tetrahedrally coordinated by the four oxygens of the four bridging bidentate carboxylate groups in a syn-anti arrangement [1]. They form two-dimensional sheets along the bc plane. The space group is C2/c or C_{2h}^6. The averaged Zn–O distance is 1.957 Å and the C–O distance is 1.252 Å. There are the four symmetry species of Au and Bu of infrared active vibrations and Ag and Bg of Raman active ones. In this study, we made a factor group analysis and a normal mode analysis on anhydrous zinc acetate crystal and assigned the vibrations of intra- and intermolecular ones. A qualitative vibrational analysis has been reported by Johnson et al. [2]. They considered that the coordination structure was a chelating bidentate form, but the structure has been revealed as a bridging bidentate one [1].

A similar crystal structure has been reported for zinc propionate $(CH_3CH_2CO_2)_2Zn$ [3]. Its crystal structure belongs to space group $P2_1/c$ in which the zinc atoms are linked by propionate groups in a syn-anti arrangement in the bc plane. The averaged Zn–O distance is 1.953 Å and the C–O distance is 1.25 Å. Hence, this coordination structure is very similar to that in monoclinic anhydrous zinc acetate. Also, zinc propionate is one of the simplest zinc soaps. The crystal structures of metal soaps are known

* Corresponding author. Tel.: +81 764 456610; fax: +81 764 456549; e-mail: ishioka@sci.toyama-u.ac.jp

1386-1425/98/$ - see front matter
PII S1386-1425(98)00061-4

only for a few compounds, i.e. two crystal forms of potassium palmitate and its high temperature phase [4–6], copper caprate and caprylate [7,8] and strontium caprate hydrate [9]. However, the crystal structure of rather common longer chain soaps such as zinc stearate have not been reported until now. The coordination structure of the carboxylate groups around a zinc atom in zinc stearate is not known.

In this study, we discuss the coordination geometry in zinc stearate based on the vibrational analysis of anhydrous zinc acetate.

2. Experimental

Anhydrous zinc acetate powder was recrystallized from dry-ethanol solution of zinc acetate dihydrate (Aldrich, 99.999%). Absence of water molecules was confirmed by an infrared spectrum. The specimen was unstable under moisture and readily changed to the dihydrate. Other anhydrous zinc acetate powders were obtained by drying zinc acetate dihydrate at 110°C over a night and at 120°C over 1 week. Dehydration of the two water molecules by drying was confirmed by a Rigaku TG-DTA 8101BH.

Zinc stearate was synthesized from sodium stearate (Sigma, 99%) in dry ethanol solution by titrating equimolar $ZnCl_2$ aq. slowly. The solution was precipitated in diethylether. The product was filtered and dried at 60°C under vacuum. These procedures were repeated $5\times$. The purity was confirmed by the IR spectrum and the elemental analysis.

X-ray powder diffractions were measured by a SHIMAZU XD-3A diffractometer with a Ni filtered Cu–K_α line of 1.5418 Å.

Infrared spectra were measured by a JASCO IR-810 spectrophotometer at room temperature. Raman spectra were obtained at 77 K by a JASCO R-800 double monochromator with an Ar^+ laser 514.5 nm excitation line and at room temperature by a JASCO RFT-200 FT-Raman spectrometer with an Nd: YAG laser 1064 nm excitation line.

3. Results and discussion

3.1. Anhydrous zinc acetate

3.1.1. Crystal structure

Anhydrous zinc acetate takes different structures by different preparation methods. Before vibrational analysis, we need to check whether a specimen have a known crystal structure. Two crystal structures of anhydrous zinc acetate have been known. One is monoclinic form in which a zinc atom is tetrahedrally coordinated by the four oxygens of the four bridging bidentate carboxylate groups, and they form two-dimensional sheets along the bc plane [1]. Another is orthorhombic form in which a zinc atom is coordinated as described above, but they form three-dimensional network [10]. The former crystal was crystallized from dry-ethanol solution of zinc acetate dihydrate, but the preparation method of the latter crystal was not reported. Fig. 1 shows three observed X-ray diffraction patterns of (a–c) and one simulated pattern of (d): (a) is a pattern of the specimen dried at 110°C over 1 night; (b) is that dried at 120°C over 1 week; (c) is crystallized from dry-ethanol solution; (d) is simulated based on the monoclinic structure. For the simulation, the 2θ values were obtained from the reported cell-dimensions and the intensities from the reported $|F_0|^2$ values where F_o's below 50 were neglected. Since intensity corrections were not made, discrepancies between observed and calculated intensities in the high 2θ region were recognized. The observed patterns (a) and (b) are clearly different from (c), but (c) coincides with (d). Hence, we confirmed to having obtained a powder specimen (c) having the monoclinic structure. The structures of (a) and (b) may be ascribed to the orthorhombic one but we did not confirm it.

3.1.2. Normal mode analysis

A normal mode analysis was made for the monoclinic specimen as follows. The Cartesian coordinates were evaluated according to the crystal structure. The CH_3 group was assumed as a unit atom. The unit cell contains eight asymmetric units. We calculated the frequencies for a primitive cell containing four asymmetry units of

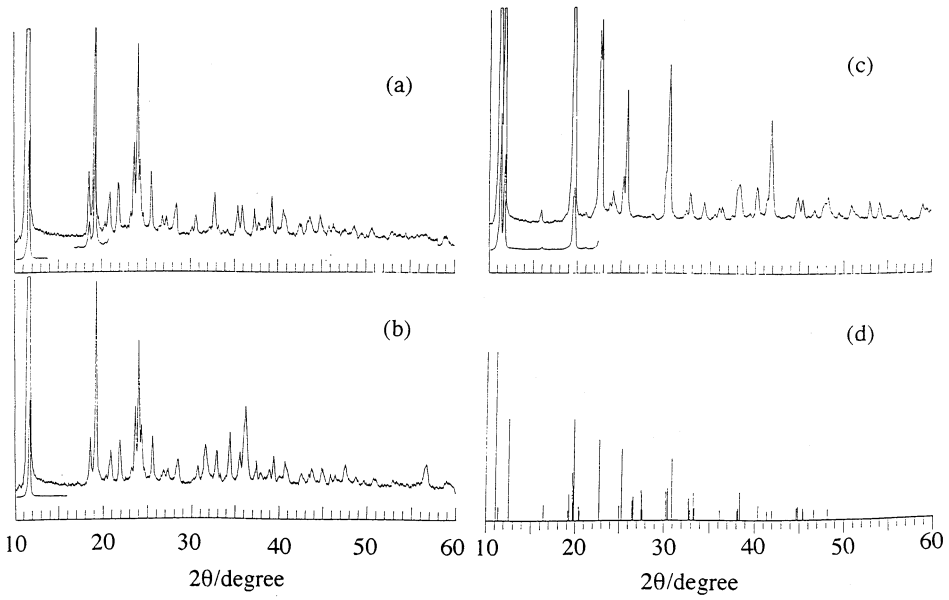

Fig. 1. X-ray powder diffraction patterns of (a) anhydrous zinc acetate obtained by drying zinc acetate dihydrate at 110°C over 1 night; (b) by drying at 120°C over 1 week; (c) by crystallized from dry-ethanol solution of zinc acetate dihydrate and (d) simulated based on the crystal structure of monoclinic anhydrous zinc acetate.

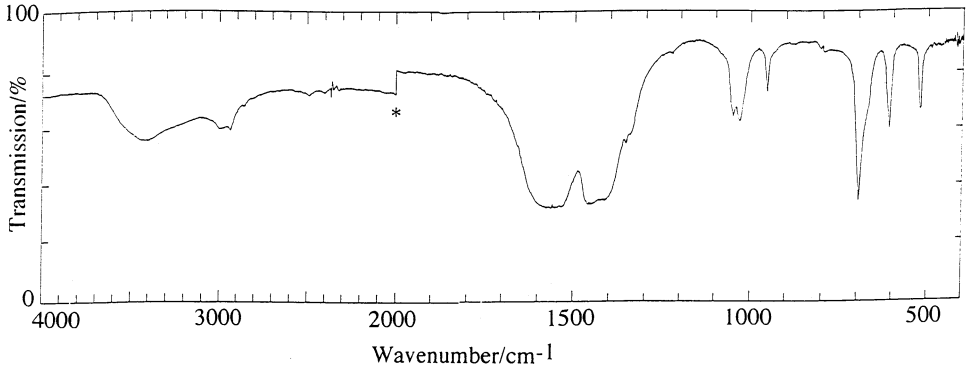

Fig. 2. Infrared spectrum of monoclinic anhydrous zinc acetate at room temperature in the 400–4000 cm^{-1} region. The asterisk is due to grating change.

$Zn(OOCCH_3)_2$ where Zn and O were assumed to be covalently bonded. The crystal belongs to the space group C2/c or C_{2h}^6. The asymmetric unit belongs to the C_2 point group and has 11A and 10B vibrations. The site symmetry is C_2. Hence, we have $(22+4R)Ag$, $(22+3T)Au$, $(20+8R)Bg$ and $(20+6T)Bu$ crystal vibrations where R and T indicate rotational and translational lattice modes, respectively. The Ag and Bg species are Raman active and the Au and Bu species are infrared active. Fig. 2 shows infrared spectrum in the 400–4000 cm^{-1} region where a broad band around 3400 cm^{-1} was confirmed to be ascribed to moisture in the KBr disc. Fig. 3 shows Raman spectrum of anhydrous zinc acetate in the 200–2000 and 2500–3500 cm^{-1} region. The valence force constants were transferred from the values of zinc acetate dihydrate [11] and were adjusted to fit both the calculated and the observed frequencies for the COO stretches, the CC stretch, the OCO bend, the CCO bend and the COO out-of-plane, as listed in Table 1. We were able to fit the

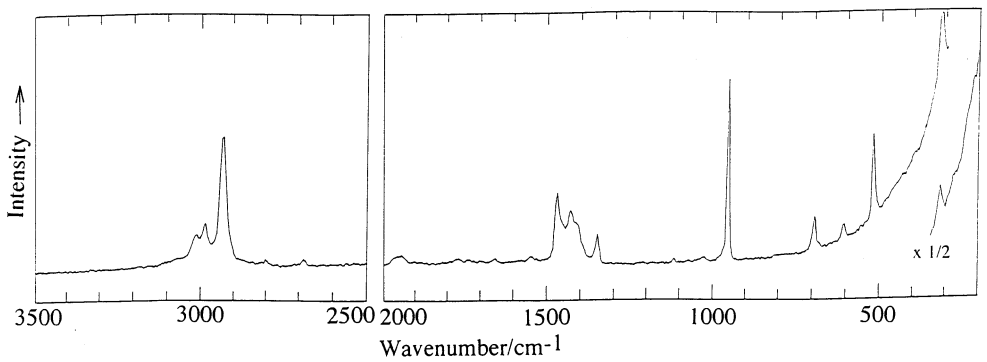

Fig. 3. Raman spectrum of monoclinic anhydrous zinc acetate at 77 K in the 200–2000 cm^{-1} and 2500–3500 cm^{-1} regions.

frequencies by adjusting a few force constants at an interval of 0.01 for one frequency, e.g. we adjusted K(O–C), H_{α}(OCO) and K(C–CH_3) for the frequency of the COO stretches, and π(COO) for the COO out-of-plane bend, by referring the result of the potential energy distributions in the zinc acetate dihydrate. The non-bonded force field was assumed as Buckingham type and was transferred from that in our normal mode analyses of $CH_3CO_2 \cdot NH_4$ and $BaCl_2 \cdot 2H_2O$ crystals [12,13] as initial values, and then adjusted by the least squares method. The cut-off distance was 5 Å. The calculation was made using an IBM RS/6000–580 computer at this university. The assignments were made with L_x vectors. The calculated frequencies agreed well with the observed ones, as listed in Table 2.

3.1.3. Spectral assignments

The assignments regarding the COO group are the same as those in the case of zinc acetate dihydrate and those reported by Johnson et al. [2]. In the infrared spectrum, 3T (Au) and 6T (Bu) and in the Raman spectrum, 4R (Ag) and 8R (Bg) should be appeared. By referring our previous normal mode analysis of ammonium acetate crystal and its deuterated compounds [12], these lattice modes are expected to appear below about 100 cm^{-1}. With using the L_x vectors, we assigned these modes and listed in Table 2. Some discrepancies of the assignments in the low frequency region were found between ours and those of Johnson et al. but precise argument was not possible since the observed bands were very few.

3.2. Zinc stearate

The monoclinic anhydrous zinc acetate has the COO modes as follows. The antisymmetric stretch at 1565 cm^{-1} (IR), the symmetric stretch at 1450 cm^{-1} (IR) and 1471 cm^{-1} (Raman), the bend at 697 cm^{-1} (IR) and 699 cm^{-1} (Raman), the out-of-plane at 612 cm^{-1} (IR and Raman), and the rock at 522 cm^{-1} (IR) and 526 cm^{-1} (Raman). On the other hand, zinc acetate dihydrate has the modes as follows [11]. The antisymmetric stretch at 1558 cm^{-1} (IR), the symmetric stretch at 1445 cm^{-1} (IR) and 1460 cm^{-1} (Raman), the bend at 696 cm^{-1} (IR) and 698 cm^{-1} (Raman), the out-of-plane at 622 cm^{-1} (IR) and 627 cm^{-1} (Raman), and the rock at 473 cm^{-1} (Raman). In zinc acetate dihydrate and anhydrous zinc acetate, the carboxylate groups have different coordination forms, i.e. the chelating bidentate and the bridging bidentate forms, respectively. The difference reflects the frequency difference of about 50 cm^{-1} in the rock. Based on this result, we examined the coordination form of zinc stearate as a typical long-chain soap.

3.2.1. Spectral assignments

Figs. 4 and 5 show the infrared spectrum of zinc stearate in the 400–1800 cm^{-1} and the Raman spectrum in the 100–2000 cm^{-1} region, respectively. In the infrared spectrum, fine structures appeared in the 700–1400 cm^{-1} region which were assigned to the methylene progressive bands. We observed three intense bands in the 1300–1600 cm^{-1} region. The 1540 cm^{-1} band is

Table 1
Valence and non-bonded force constants of $Zn(CH_3CO_2)_2$

	Force constants[a]				Force constants		
	Initial	Final	Bond distance (Å)		Initial	Final	Bond distance (Å)
K(Zn···Zn)	0.340	0.340	4.651		0.002	0.002	3.565
K(Zn–O)	1.500	1.300	1.951		0.001	0.001	3.626
	1.293	1.293	1.953	$K(O\cdots CH_3)$	0.730	0.350	2.351
	1.275	1.275	1.958		0.350	0.350	2.366
	1.255	1.255	1.965		0.350	0.350	2.390
K(Zn···O)	0.154	0.154	2.785		0.350	0.350	2.392
	0.100	0.100	2.953		0.010	0.010	3.165
K(Zn···C)	0.500	0.200	2.708		0.010	0.010	3.363
	0.164	0.164	2.780		0.010	0.010	3.573
	0.113	0.113	2.920		0.010	0.010	3.765
	0.100	0.100	2.964		0.010	0.010	3.947
$K(Zn\cdots CH_3)$	0.050	0.050	3.268	K(C···C)	0.100	0.070	3.606
	0.050	0.050	3.410	$K(C-CH_3)$	4.850	5.000	
K(O···O)	0.940	0.500	2.175		4.850	5.000	
	0.497	0.497	2.189	$K(CH_3\cdots CH_3)$	0.800	0.100	3.281
	0.324	0.324	3.019		0.082	0.082	3.533
	0.314	0.314	3.084		0.053	0.053	4.072
	0.303	0.303	3.154		0.050	0.050	4.155
	0.301	0.301	3.164	H(O–Zn–O)	0.100	0.100	
	0.300	0.300	3.172	H_β(CCO)	0.620	0.500	
K(O–C)	9.420	8.000		H_α(OCO)	1.750	1.250	
	9.420	8.000		H(COZn)	0.100	0.100	
	9.420	8.000		π(COO)	0.205	0.610	
	9.420	8.000		F_r(COO)	1.640	1.500	
K(O···C)	0.005	0.005	3.446	F_{Rr}(COO)	0.160	0.160	
	0.004	0.004	3.459	$F_{r\alpha}$	1.246	1.246	
	0.003	0.003	3.501	$F_{r\beta}$(COO)	0.280	0.280	
	0.003	0.003	3.509	$F_{R\beta}$(COO)	0.515	0.400	
	0.002	0.002	3.554				

[a] Stretching constants (K) are in units of mdyn/Å, bendings (H) are of mdyn Å/rad^2, and out-of-plane (π) is of mdyn Å.

assigned to the carboxylate antisymmetric stretch and 1465 cm^{-1} to the CH_2 bending by referring to our assignments of potassium soaps [14–16]. The 1399 cm^{-1} band may be assigned to the $C_\alpha H_2$ bending and/or the carboxylate symmetric stretch, both of which should be observed in the infrared spectrum. In the Raman spectrum, five intense bands appeared at 1067, 1134, 1299, 1443 and 1462 cm^{-1}. The 1067 and 1134 cm^{-1} bands were assigned to the antisymmetric and symmetric CC stretches, respectively [17]. The 1299 cm^{-1} to the CH_2 twist. The CH_2 bending region was rather complicated. The 1443 and 1462 cm^{-1} bands were assigned by referring the well-established vibrations of the polymethylene chain [17,18]. In the case of the polymethylene chain, these two bands were caused by Fermi resonance between the fundamental CH_2 bending of the phase difference $\phi = 0$ at 1442 cm^{-1} and the overtone of the CH_2 rocking of $\phi = \pi$ at 722 cm^{-1}. In this case of zinc stearate, the frequency of the fundamental CH_2 bending might be somewhat higher. In the long-chain compounds, the alkyl chains usually packed in a small periodic structure within the real unit cell. This small periodic structure is called as subcell. There are typically two types of subcell which have parallel and perpendicular forms of lateral chain packing. In the perpendicular case, we observe the correlation split in the subcell for the CH_2 bending and

Table 2
Observed and calculated frequencies (cm^{-1}) of $Zn(CH_3CO_2)_2$

$\nu_{obs.}$	$\nu_{calc.}$	Assignment	$\nu_{obs.}$	$\nu_{calc.}$	Assignment[a]
IR (u mode)					
3000		$\nu_{as}(CH_3)$	522	519 Bu	γ(COO)
			522	511 Au	γ(COO)
2940		$\nu_s(CH_3)$		369 Au	$\nu(ZnO_4)$
1565	1566 Au	ν_a(COO)		361 Bu	$\nu(ZnO_4)$
1565	1566 Bu	ν_a(COO)		348 Au	$\nu(ZnO_4)$
1565	1560 Au	ν_a(COO)		341 Bu	$\nu(ZnO_4)$
1565	1560 Bu	ν_a(COO)		316 Au	$\nu(ZnO_4)$
1450	1450 Au	ν_s(COO)		300 Bu	$\nu(ZnO_4)$
1450	1450 Bu	ν_s(COO)		299 Au	$\nu(ZnO_4)$
1450	1444 Au	ν_s(COO)		292 Bu	$\nu(ZnO_4)$
1450	1443 Bu	ν_s(COO)		240 Bu	$\nu(ZnO_4)$
1415		$\delta_{as}(CH_3)$		229 Au	$\nu(ZnO_4)$
1343		$\delta_s(CH_3)$		222 Au	$\nu(ZnO_4)$
1050		CH_3 rock		207 Au	$\nu(ZnO_4)$
1032		CH_3 rock		204 Bu	δ(OZnO)
955	958 Au	R(CC)		172 Bu	δ(OZnO)
955	958 Bu	R(CC)		150 Au	δ(OZnO)
955	950 Bu	R(CC)		137 Au	δ(OZnO)
955	946 Au	R(CC)		135 Bu	T
697	717 Au	α(COO)		122 Au	δ(OZnO)
697	717 Bu	α(COO)		122 Bu	T
697	704 Au	α(COO)		109 Au	δ(OZnO)
697	698 Bu	α(COO)		108 Bu	T
612	617 Au	π(COO)		85 Au	T
612	606 Bu	π(COO)		68 Bu	T
612	605 Au	π(COO)		59 Au	T
612	603 Bu	π(COO)		51 Bu	T
522	542 Bu	γ(COO)		47 Au	T
522	534 Au	γ(COO)		27 Bu	T
Raman (g mode)					
3023		$\nu_{as}(CH_3)$		362 Ag	$\nu(ZnO_4)$
2995		$\nu_{as}(CH_3)$		348 Bg	$\nu(ZnO_4)$
2941		$\nu_s(CH_3)$		343 Ag	$\nu(ZnO_4)$
	1567 Bg	ν_a(COO)	321	319 Bg	$\nu(ZnO_4)$
	1566 Ag	ν_a(COO)		301 Ag	$\nu(ZnO_4)$
	1560 Ag	ν_a(COO)		300 Bg	$\nu(ZnO_4)$
	1560 Bg	ν_a(COO)		298 Ag	$\nu(ZnO_4)$
1471	1450 Ag	ν_s(COO)		242 Ag	$\nu(ZnO_4)$
1471	1450 Bg	ν_s(COO)		228 Bg	$\nu(ZnO_4)$
1471	1444 Bg	ν_s(COO)	217	218 Bg	$\nu(ZnO_4)$
1471	1443 Ag	ν_s(COO)		213 Ag	$\nu(ZnO_4)$
1433		$\delta_{as}(CH_3)$		207 Bg	δ(OZnO)
1415		$\delta_{as}(CH_3)$		174 Ag	δ(OZnO)
1354		$\delta_s(CH_3)$			
958	958 Ag	R(CC)		146 Ag	δ(OZnO)
958	958 Bg	R(CC)		142 Bg	R
958	954 Ag	R(CC)		134 Ag	δ(OZnO)
958	950 Bg	R(CC)		132 Bg	R
699	719 Ag	α(COO)		119 Bg	R
699	719 Bg	α(COO)		115 Ag	δ(OZnO)

Table 2 *(Continued)*

$\nu_{obs.}$	$\nu_{calc.}$	Assignment	$\nu_{obs.}$	$\nu_{calc.}$	Assignment[a]
699	704 Bg	α(COO)		102 Bg	R
699	699 Ag	α(COO)		82 Bg	R
612	616 Ag	π(COO)		76 Ag	δ(OZnO)
612	614 Bg	π(COO)		63 Ag	R
612	611 Ag	π(COO)		53 Bg	R
612	603 Bg	π(COO)		52 Ag	R
526	544 Ag	γ(COO)		37 Bg	R
526	533 Bg	γ(COO)		36 Ag	R
526	521 Ag	γ(COO)		25 Bg	R
526	509 Bg	γ(COO)		22 Ag	R
	368 Bg	$\nu(ZnO_4)$			

Observed, obs.; calculated, calc.

[a] The symbols are the same as part 1 of this series. T and R indicate translational and rotational lattice vibrations, respectively.

the CH_2 rocking regions, but in the parallel case we do not observe it. In this case of zinc stearate, we did not observe the split in the CH_2 bending and rocking regions, and therefore the subcell was parallel type. We found the 1403 cm^{-1} band in the Raman spectrum. This was not the split component of the CH_2 bending in a perpendicular type subcell which should appear at 1416 cm^{-1}. Usually, the intensity of the $C_\alpha H_2$ bend is very weak in the Raman spectrum. Hence, the Raman 1403 cm^{-1} band was ascribed to the carboxylate symmetric stretch. Therefore, the 1399 cm^{-1} infrared band is considered to be an overlapped bands of the carboxylate symmetric stretch and the $C_\alpha H_2$ bend. In the infrared spectrum, the carboxylate bend was observed at 744 cm^{-1}. The carboxylate out-of-plane and the rock appeared at 579 and 548 cm^{-1}, respectively. These assignments were consistent with our ones for potassium soaps.

3.2.2. Coordination structure

The carboxylate antisymmetric and symmetric stretch of zinc stearate appeared apart from those of zinc acetates ~ 10 cm^{-1}. Hence, the force field around the zinc atom in zinc stearate is somewhat different from those in zinc acetates. However, the rock which is the key band to determine the coordination structure, appeared at almost the same frequency with that of the monoclinic zinc acetate anhydride. Hence, we considered the coordination structure in the zinc stearate may be the same as the monoclinic anhydrous zinc acetate, i.e. the bridging bidentate.

An EXAFS study pointed out that the averaged Zn–O (carboxylate) length reflects the coordination structure around the zinc atom [19]. Zinc acetate dihydrate has the averaged length of 2.188 (4) Å, monoclinic anhydrous zinc acetate 1.957 (2), orthorhombic anhydrous zinc acetate 1.934 (11), zinc propionate 1.953. Among these, only

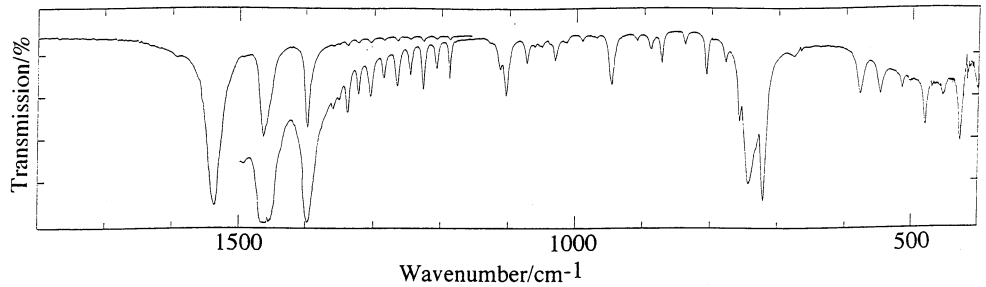

Fig. 4. Infrared spectrum of zinc stearate at room temperature in the 400–1800 cm^{-1} region.

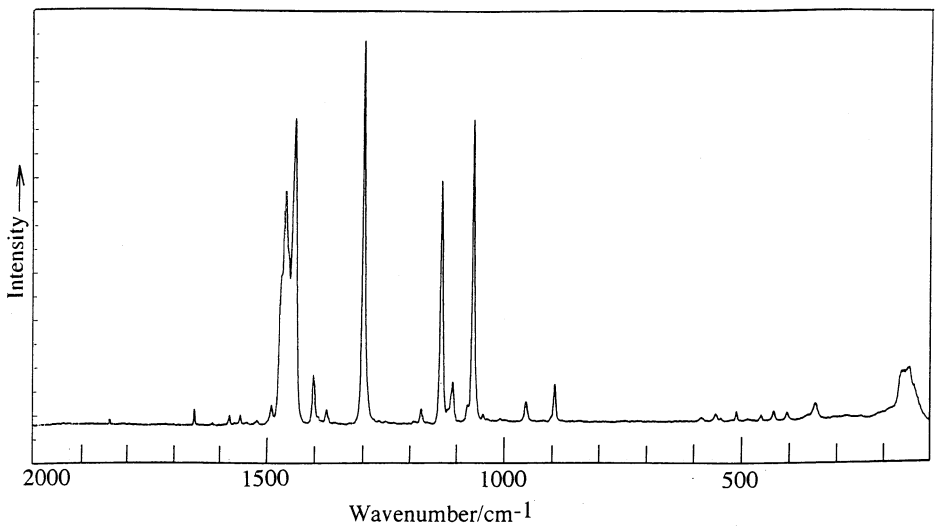

Fig. 5. Raman spectrum of zinc stearate at room temperature in the 100–2000 cm^{-1} region.

1.95 Å by an EXAFS experiment [20]. This value closely agreed with the values of anhydrous zinc acetates and zinc propionate which have the bridging bidentate coordination forms. Hence, we conclude that the coordination structure around the zinc atom in zinc stearate is the bridging bidentate form.

Acknowledgements

We are indebted to Professor Osamu Takayasu of Toyama University for kind help of X-ray powder diffraction measurements.

References

[1] W. Clegg, I.R. Little, B.P. Straughan, Acta Crystallogr. C42 (1986) 1701.
[2] M.K. Johnson, D.B. Powell, R.D. Cannon, Spectrochim. Acta 37A (1981) 899.
[3] E. Goldschmied, A.D. Rae, N.C. Stephenson, Acta Crystallogr. B33 (1977) 2117.
[4] J.H. Dumbleton, T.R. Lomer, Acta Crystallogr. 19 (1965) 301.
[5] E.L.V. Lewis, T.R. Lomer, Acta Crystallogr. B25 (1969) 702.
[6] D.M. Glover, Acta Crystallogr. A37 (1981) 251.
[7] T.R. Lomer, K. Perera, Acta Crystallogr. B30 (1974) 2912.
[8] T.R. Lomer, K. Perera, Acta Crystallogr. B30 (1974) 2913.
[9] E. Stanley, Nature 203 (1964) 1375.
[10] A.V. Capilla, R.A. Aranda, Cryst. Struct. Comm. 8 (1979) 795.
[11] T. Ishioka, Y. Shiobata, M. Takahashi, I. Kanesaka, Y. Kitagawa, K.T. Nakamura, Spectrochim. Acta (1998) in press.
[12] I. Kanesaka, H. Tanbo, H. Kawahara, K. Kawai, J. Raman Spectrosc. 16 (1985) 297.
[13] I. Kanesaka, T. Matsuda, Y. Niwa, J. Raman Spectrosc. 25 (1994) 245.
[14] T. Ishioka, Bull. Chem. Soc. Jpn. 64 (1991) 2174.
[15] T. Ishioka, S. Murotani, I. Kanesaka, S. Hayashi, J. Chem. Phys. 103 (1995) 1999.
[16] T. Ishioka, I. Kanesaka, Polym. J. 26 (1994) 643.
[17] M. Kobayashi, H. Tadokoro, R.S. Porter, J. Chem. Phys. 73 (1980) 3635.
[18] R.G. Snyder, S.L. Hsu, S. Krimm, Spectrochim. Acta 34A (1978) 395.
[19] H.K. Pan, G.S. Knapp, S.L. Cooper, Colloid Polym. Sci. 262 (1984) 734.
[20] T. Ishioka, I. Watanabe, M. Harada, S. Kawauchi, Photon factory activity report, National laboratory for high energy physics, Japan 13 (1995) 175.